Automatic Classification and Retrieval of Brain Hemorrhages

Hau Lee Tong[1], Mohammad Faizal Ahmad Fauzi[2], Su Cheng Haw[1], Hu Ng[1] and Timothy Tzen Vun Yap[1]

[1]Faculty of Computing and Informatics, Multimedia University, 63100 Cyberjaya, Selangor, Malaysia
[2]Faculty of Engineering, Multimedia University, 63100 Cyberjaya, Selangor, Malaysia
hltong@mmu.edu.my

Abstract. In this work, Computed Tomography (CT) brain images are adopted for the annotation of different types of hemorrhages. The ultimate objective is to devise the semantics-based retrieval system for retrieving the images based on the different keywords. The adopted keywords are hemorrhagic slices, intra-axial, subdural and extradural slices. The proposed approach is consisted of three separated annotation processes are proposed which are annotation of hemorrhagic slices, annotation of intra-axial and annotation of subdural and extradural. The dataset with 519 CT images is obtained from two collaborating hospitals. For the classification, support vector machine (SVM) with radial basis function (RBF) kernel is considered. On overall, the classification results from each experiment achieved precision and recall of more than 79%. After the classification, the images will be annotated with the classified keywords together with the obtained decision values. During the retrieval, the relevant images will be retrieved and ranked correspondingly according to the decision values.

Keywords: Brain Hemorrhages, Image Classification, Image Retrieval.

1 Introduction

Intracranial hemorrhage detection is clinically significant for the patients having head trauma and neurological disturbances. This is because early discovery and accurate diagnosis of the brain abnormalities is crucial for the execution of the successful therapy and proper treatment. Multi-slice CT scans are extensively utilized in today's analysis of head traumas due to its effectiveness to unveil some abnormalities such as calcification, hemorrhage and bone fractures.

A lot of research works have been carried out to assist the visual interpretation of the medical brain images. Brain hemorrhage can cause brain shift and make it lose its symmetric property. As such, investigation of the symmetric information can assist in hemorrhage detecting. Chawla et al. proposed the detection of line of symmetry based on the physical structure of the skull [1]. Likewise, Saito et al. proposed a method to detect the brain lesion based on the difference values of the extracted features be-

R. Alfred et al. (eds.), *Computational Science and Technology*, Lecture Notes in Electrical Engineering 481, https://doi.org/10.1007/978-981-13-2622-6_1

tween region of interests (ROIs) at symmetrical position [2]. The symmetric line is determined from the midpoints of the skull contour. Besides the symmetric detection approach, segmentation technique is commonly adopted to obtain the potential desired regions. Bhadauria and Dewal proposed an approach by combining the features of both fuzzy c-means and region-based active contour method to segment the hemorrhagic regions [3]. Al-Ayyoub et al. used Otsu's thresholding method for the image segmentation [4]. From the Otsu's method, the potential ROIs are obtained. Jyoti et al. proposed genetic FCM (GFCM), a clustering algorithm integrated with Genetic Algorithm (GA) to segment the CT brain images with the modified objective function [5]. Suryawanshi and Jadhao adopted a neural network approach with watershed segmentation to detect the intracerebral haemorrhage and subdural [6].

Huge collections of medical images have contributed significant source of knowledge and various areas of medical research. However, the major problem is that the size of the medical image collection in hospitals faces constant daily growth. Thus the amount of work and time required for retrieving a particular image for further analysis is costly. As such, image retrieval particularly in medical domain has gained some attention in the research area of content-based image retrieval (CBIR) [7-10].

Consequently, multi-slice CT brain images are adopted in this work to classify, annotate and retrieve the images by using different keywords based on the type of hemorrhages. The retrieval is based on the adopted keywords which are hemorrhagic slices, intra-axial, subdural and extradural slices

2 Proposed System Overview

The architecture diagram of our proposed system is shown in Fig. 1. The proposed system consists of two main components, i.e., the offline mode and online mode. The offline component will be the automated annotation part. Each CT scan will be annotated by the keywords and the attached semantic keyword will be stored into a database. On the other hand, the online component will be the retrieval part. CT images can be retrieved according to the predefined keywords.

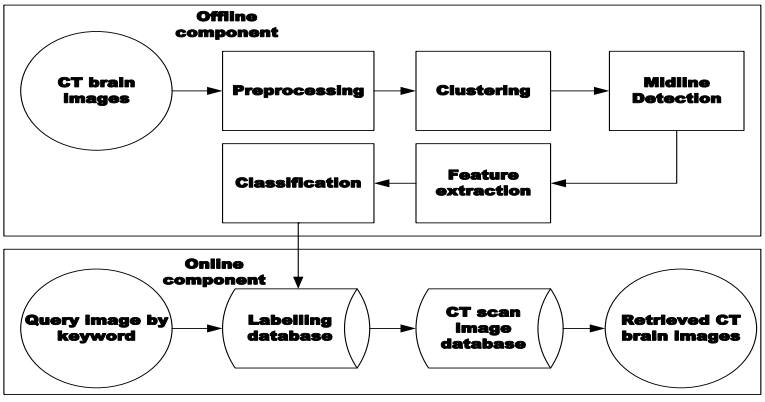

Fig. 1. Overview of proposed annotation and retrieval

3 Preprocessing

3.1 Original Image Enhancement

The original CT images are lacking in dynamic range whereby only limited objects are visible. The major aim of the enhancement is to augment the interpretability and perception of images to contribute better input for the subsequent image processing process. Firstly the histogram for the original image is constructed as shown in Fig. 2(a). The constructed histogram is consisted of several peaks. However, only the rightmost peak is within the significant range for region of interest which is the intracranial area. Then, the curve smoothing process is conducted where convolution operation with a vector is applied. Each element of the vector is of the value 10^{-3}. The smoothened curve is converted into absolute first difference (ABS) in order to generate two highest peaks. The two generated peaks will be the lower limit, I_L and upper limit, I_U. The acquired I_L and I_U are utilized for the linear contrast stretching as shown in equation (1).

$$F(i,j) = I_{\max} \frac{(I(i,j) - I_L)}{(I_U - I_L)} \tag{1}$$

where Imax, $I(i,j)$ and $F(i,j)$ denote the maximum intensity of the image, pixel value of the original image and pixel value of the contrast improved image respectively. After contrast stretching, the contrast enhanced image is shown in Fig. 2(b).

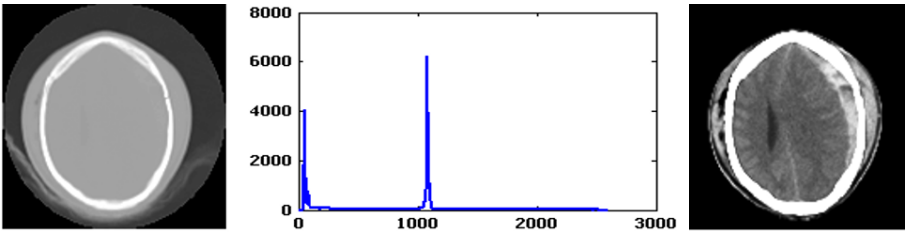

(a) (b) (c)

Fig. 2. (a) Original Image (b) Histogram of the original image (b) Enhanced Image

3.2 Parenchyma Extraction

The subsequent preprocessing is to extract the parenchyma from the enhanced image. In order to obtain the parenchyma, thresholding technique is employed to isolate the background, skull and scalp from it. Usually, the skull always appears to be the largest connected component compared with the objects in the background. Therefore, the largest connected component is identified in order to detect the skull. Subsequently, parenchyma mask is generated by filling up the hole inside the skull. Finally, intensity of the skull is set to zero and the acquired parenchyma is shown in Fig. 3.

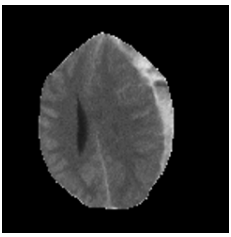

Fig. 3. The acquired parenchyma

3.3 Potential Hemorrhagic Regions Contrast Enhancement

The purpose of third preprocessing is to further enhance the parenchyma for the subsequent clustering stage. Thus, this enhancement aim to make the hemorrhagic regions more visible to clearly reveal the dissimilarity between the hemorrhagic hemisphere and non-hemorrhagic hemisphere. Prior to contrast stretching, the appropriate lower and upper limits need to be obtained. Firstly construct the histogram for the acquired parenchyma. Then identify the lower limit, I_L which is the peak position of the constructed histogram. From the obtained lower limit, the upper limit can be derived by equation (2). The determination of the appropriate lower and upper limits is necessary to ensure the focus of the stretching is for the hemorrhagic regions rather than normal regions.

$$I_U = I_L + Ie \tag{2}$$

where Ie is predefined at 500 as found from experimental observation.

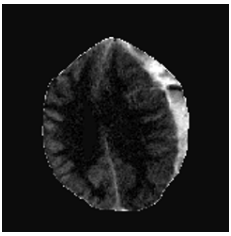

Fig. 4. Hemorrhagic region contrast enhanced image

Lastly, input the auto-determined values of I_L and I_U into equation (1) for the contrast stretching and the result is depicted in Fig. 4.

4 Potential Hemorrhagic Region Clustering

The main goal for this section is to garner potential hemorrhagic regions into a single cluster to be used for the annotation of the hemorrhages. Hemorrhagic regions always appear as bright regions. Therefore only intensity of the images is considered for the

clustering. In order to achieve this, firstly, the image is partitioned into two clusters. From these two clusters, the low intensity cluster without potential hemorrhagic regions is ignored. Only the high intensity cluster which consists of potential hemorrhagic regions is considered. Four clustering techniques which are Otsu thresholding, fuzzy c-means (FCM), k-means and expectation-maximization (EM) are attempted in order to select the most appropriate technique for subdural, extradural and intra-axial hemorrhages annotation.

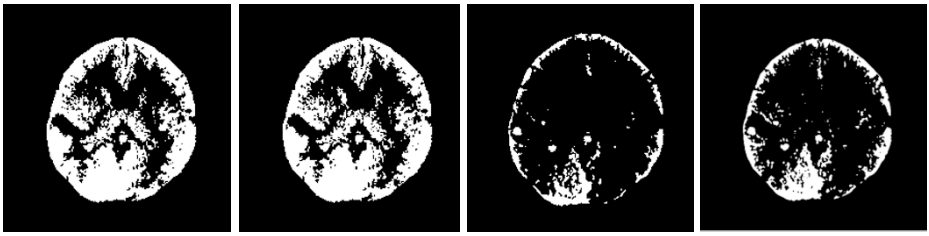

(a) (b) (c) (d)

Fig. 5. Clustering results by (a) Otsu thresholding (b) FCM clustering (c) K-means clustering and (d) EM clustering

From the results obtained as shown in Fig. 5, Otsu thresholding, FCM and EM encountered over-segmentation as hemorrhagic region is merged together with neighbouring pixels and more noises are present. On the other hand, k-means conserves the appropriate shape most of the time and yields less noise. This directly contributes to more precise shape properties acquisition at the later region-based feature extraction. Consequently, k-means clustering is adopted in our system.

5 Midline detection

The proposed approach of the parenchyma midline acquisition consists of two stages. Firstly, acquire the contour of the parenchyma as shown in Fig. 6(a). Then the line scanning process will be executed: The scanning begins from the endpoints of the top and bottom sub-contours to locate the local minima and local maxima for top and bottom sub-contour respectively. The line scanning of local maxima, (x_1,y_1) for bottom sub-contour is as illustrated in Fig. 6(d).

In the case where the local minima or maxima point is not detected, Radon transform [11] will be utilized to shorten the searching line. Radon transform is defined as:

$$R(\rho,\theta) = \iint f(x,y)\delta(\rho - x\cos\theta - y\sin\theta)dxdy \tag{3}$$

where ρ,θ and $f(x,y)$ denote distance from origin to the line, angle from the X-axis to the normal direction of the line and pixel intensity at coordinate (x,y). Dirac delta function is the obtained shortened line is thickened as depicted in Fig. 6(e).

Then moving average is applied to locate the points of interest, (x_2,y_2) from the shortened contour line. Basically moving average is used for the computation of the

average intensity for all the points along the contour line. The location of the points is based on the highest average value of intensity as shown in Fig. 6 (f).

Eventually, midline is formed by using the linear interpolation as defined in equation (4). The detected midlines are shown in Fig. 7.

$$y = y_1 + \frac{(x - x_1)(y_2 - y_1)}{(x_2 - x_1)} \tag{4}$$

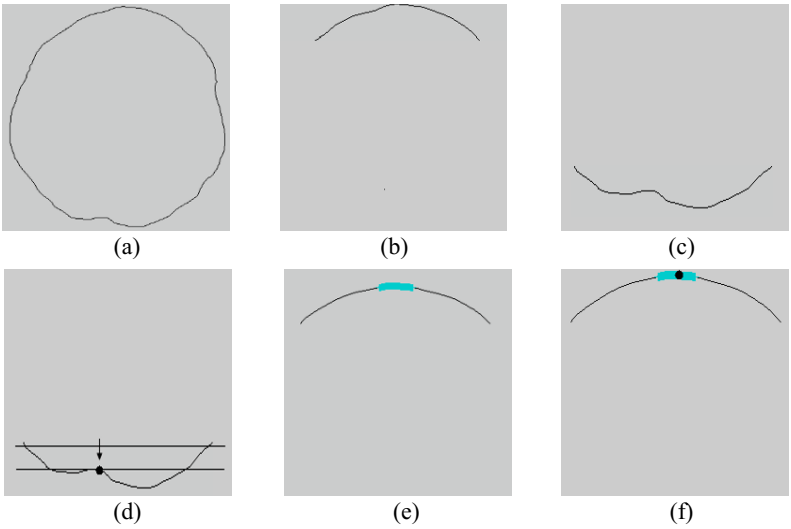

Fig. 6. (a) Contour of parenchyma area (b) Top sub-contour (c) Bottom sub-contour (d) Line scanning for local maxima detection (e) Shortened searching line (f) Located highest average value of intensity point

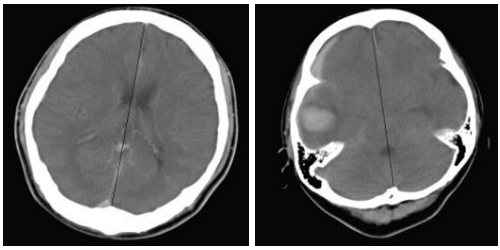

Fig. 7. The detected midline

6 Feature Extraction

Features are extracted from the left and right hemispheres and used to classify the images. There is a three-stage feature extraction which is feature extraction for hemorrhagic slices, feature extraction for intra-axial slices and feature extraction for sub-

dural and extradural. Twenty three features are proposed based on their ability to distinguish hemorrhagic and non-hemorrhagic slices. These twenty three features are derived based on one feature from Local Binary Pattern (LBP), one from entropy, four from four-bin histogram, one from intensity histogram and sixteen from four Haralick texture features(energy, entropy, autocorrelation and maximum probability) descriptors on four directions. Prior to the feature extraction for intra-axial, subdural and extradural, the potential hemorrhagic regions will be divided into intra regions and boundary regions. Intra regions will proceed with the intra-axial feature extraction with the twenty three that identical with the features of hemorrhagic slices. On the other hand, the boundary regions will proceed with the region-based feature extraction to annotate the subdural and extradural. The twelve shape features adopted are region area, border contact area, orientation, linearity, concavity, ellipticity, circularity, triangularity, solidity, extent, eccentricity and sum of centroid contour distance curve Fourier descriptor(CCDCFD). Some of the adopted shape features are defined in equation (4) to equation (8)

Linearity, $$L(ROI) = 1 - \frac{\text{minor axis}}{\text{major axis}} \tag{5}$$

Triangularity, $$\angle(ROI) = \begin{cases} 108I & if\ I \le \frac{1}{108} \\ \frac{1}{108I} & otherwise \end{cases}, \tag{6}$$

Where $I = \frac{\mu_{2,0}(ROI)\mu_{0,2}(ROI) - (\mu_{1,1}(ROI))^2}{(\mu_{0,0}(ROI))^4}$ and $\mu_{i,j}(ROI)$ is the (i,j)-moment

Ellipticity, $$1(ROI) = \begin{cases} 16\pi^2 I & if\ I \le \frac{1}{16\pi^2} \\ \frac{1}{16\pi^2 I} & otherwise \end{cases}, \tag{7}$$

Circularity, $$\partial(ROI) = \frac{(\mu_{0,0}(ROI))^2}{2\pi(\mu_{2,0}(ROI) + \mu_{0,2}(ROI))} \tag{8}$$

Sum of CCDC= $$\sum_{k=2}^{N-1} \left| \frac{ft(k)}{ft(1)} \right| \tag{9}$$

Where $ft(k) = \frac{1}{N}\sum_{n=0}^{N-1} z(n) \exp\left(\frac{-i2\pi kn}{N}\right)$, k=0, 1, 2…., N-1, $z(n) = x_1(n) + iy_1(n)$ and

contour points= $(x_1(n), y_1(n))$.

Region area, border contact area and orientation are employed to differentiate the normal regions from the subdural and extradural regions. The subsequent eight features are primarily adopted to differentiate extradural from subdural. Extradural and subdural always appear to be bi-convex and elongated crescent in shape respectively. Generally, extradural is more solid, extent, elliptic, circular and triangular as compared to subdural. However, subdural is more concave and linear than extradural.

7 Classification

The acquired CT brain images are in DICOM format with their dimension 512 x 512. The images are acquired from two collaborating hospitals, which are Serdang Hospital and Putrajaya Hospital, to test the feasibility of the proposed approach on datasets generated from different scanners and different setup. The dataset consists of 181 normal slices, 209 intra-axial slices, 60 extradural slices and 86 subdural slices. The adopted classification technique is SVM with RBF kernel. During the classification, ten-fold cross validation method is performed. The features obtained from three separate feature extraction process are channel into the classifier respectively in order to categorize the different slices. The obtained recall and precision are shown in Table 1. The recall and precision for all slices achieved satisfactory results with at least 0.79 for all. This is contributed by the features employed as they well describe the characteristics of the different slices. However, the recall for intra-axial slice is relatively lower compared with other slices. Some bright normal regions presented in non-intra-axial slices increase the similarity of the features between some non-intra-axial and intra-axial slices. Therefore, it generated the higher misclassification of intra-axial slices.

Table 1. Recall and precision for different types of slices.

	Recall	Precision
Normal slice	0.917	0.834
Hemorrhagic slice	0.902	0.953
Intra axial slice	0.793	0.925
Extradural	0.850	0.927
Subdural	0.892	0.858

8 Retrieval Results

This section presents the retrieval results based on the keywords which are “hemorrhage”, “intra-axial”, “subdural” and “extradural”. The retrieval results for each keyword are exhibited based on the twenty five most relevant as shown in Fig. 8. The relevancy or ranking is based decision values obtained from RBF SVM.

Besides the visual retrieval results, the accuracy of the retrieval is evaluated based on the numbers of most relevant to the adopted keywords over 519 images. The testing numbers for each keyword are different as the evaluation is according to the number of total slices of each keyword. From Table 2, the retrieval result based on the keyword “hemorrhage” is 96% for the 300 most relevant retrievals. In this case, there are 12 irrelevant images being retrieved together in the top 300. On the other hand, for the 100 most intra-axial relevant results, there are three irrelevant images being retrieved. For 50 most extradural relevant retrieval results, the accuracy obtained is 96%. There are 2 irrelevant images presented in the retrieval results. Lastly for the 50 most subdural relevant retrieval results, the accuracy obtained is 92%. There are 4 irrelevant images being retrieved in this retrieval.

9 Conclusion

This research work proposed three segregated feature extraction processes to classify and retrieve the different types of slices based on their different features and locations. By individualizing each of the process, the appropriate approach such as midline approach, global-based and region-based feature extractions can be adopted at each level for the categorization of specific hemorrhage. Overall, the precision and recall rates are over 79% for all the classification results. In our future work, we would like to extend classification types and retrieval keywords to include more abnormalities of brain such as infarct, hydrocephalus and atrophy.

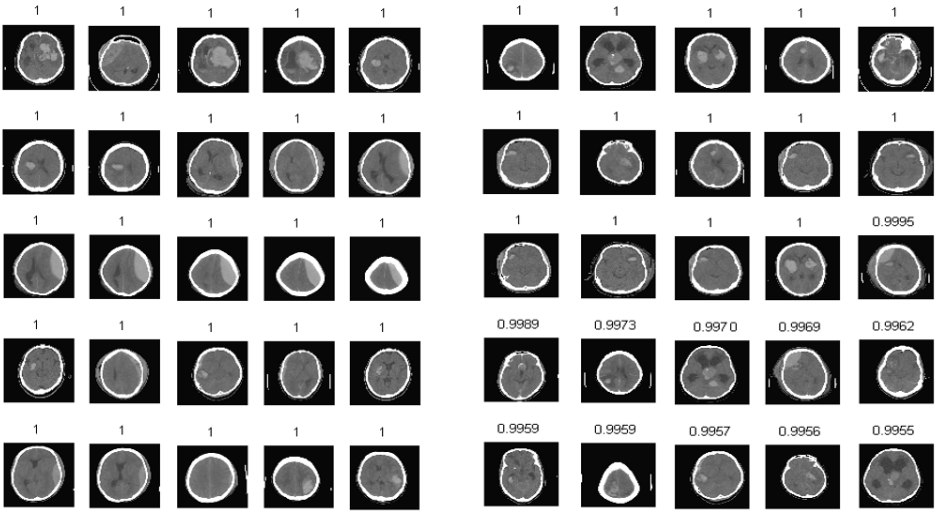

(a) Hemorrhage (b) Intra-axial

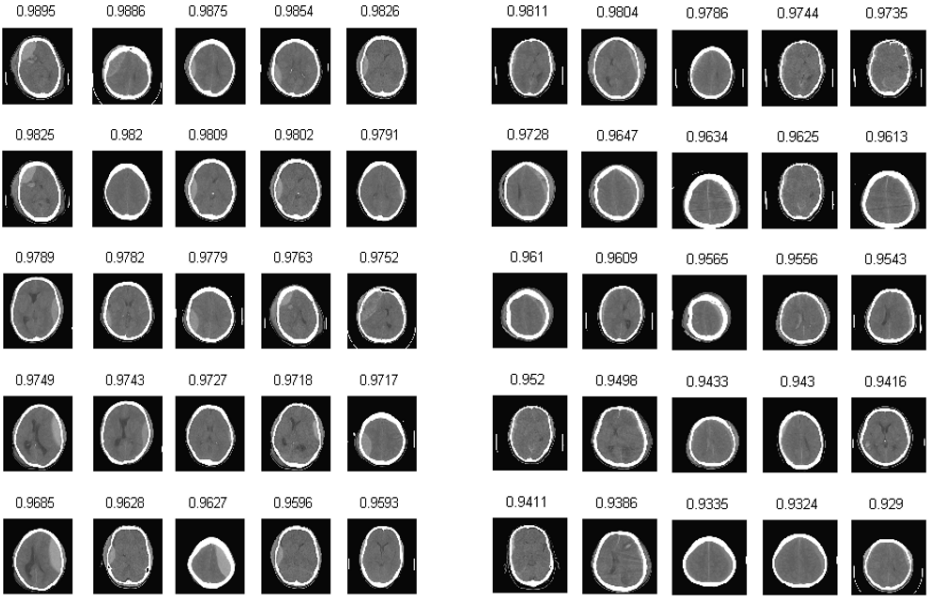

(c) Extradural (d) Subdural

Fig. 8. Twenty five most relevant retrieval results

Table 2. Retrieval accuracy by using different keywords

Numbers of most relevant retrieval	Hemorrhage	Intra-axial	Extradural	Subdural
25	100.0%	100.0%	100.0%	100.0%
50	98.0%	96.0%	96.0%	92.0%
100	99.0%	97.0%		
200	99.5%			
300	96.0%			

References

1. Chawla, M., Sharma, S., Sivaswamy, J., Kishore, L. T.: A method for automatic detection and classification of stroke from brain ct images. Annual International Conference of the IEEE Engineering in Medicine and Biology Society, pp. 3581-3584. (2009).
2. Saito, H., Katsuragawa, S., Hirai, T., Kakeda, S., Kourogi, Y.: A computerized method for detection of acute cerebral infarction on ct images. Nippon Hoshasen Gijutsu Gakkai Zasshi 66(9), 1169–1177.(2010).
3. Bhadauria, H. S., Dewal, M. L.: Intracranial hemorrhage detection using spatial fuzzy c-mean and region-based active contour on brain CT imaging. Signal, Image and Video Processing 8(2), 357-364 (2014).

4. Al-Ayyoub, M., Alawad, D., Al-Darabsah, K., Aljarrah, I.: Automatic detection and classification of brain hemorrhages. WSEAS Transactions on Computers 12(10), 395-405 (2013).
5. Jyoti, A., Mohanty, M., Kar, S., Biswal, B.: Optimized clustering method for CT brain image segmentation. Advances in Intelligent Systems and Computing 327(1),317-324. (2015).
6. Suryawanshi, S. H.,Jadhao, K. T.: Smart brain hemorrhage diagnosis using artificial neural networks. International Journal of Scientific and Technology Research 4(10), p267-271 (2015).
7. Müller, H., Deserno, T.: Content-based medical image retrieval. Biomedical image processing, biological and medical physics, biomedical engineering, pp. 471–494. (2011).
8. Ramamurthy, B., Chandran, K., Aishwarya, S., Janaranjani, P.: CBMIR: content based image retrieval using invariant moments, glcm and grayscale resolution for medical images. European Journal of Scientific Research 59(4), 460-471 (2011).
9. Müller, H., de Herrera, A., Kalpathy-Cramer, J., Demner-Fushman, D., Antani, S., Eggel, I.: Overview of the ImageCLEF 2012 medical image retrieval and classification tasks. CLEF Online Working Notes, pp. 1–16. (2012).
10. de Herrera, A. G., Kalpathy-Cramer, J., Fushman, D. D., Antani, S., Muller, H.: Overview of the ImageCLEF 2013 medical tasks. Working notes of CLEF, pp. 1-15. (2013).
11. Chen, B., Zhong, H.: line detection in image based on edge enhancement. Second International Symposium on Information Science and Engineering, pp. 415-418. IEEE Computer Society Washington, DC, USA (2009).